ELSEVIER

Journal of Chromatography A, 708 (1995) 1–12

JOURNAL OF CHROMATOGRAPHY A

Shock layer analysis for a single-component in preparative elution chromatography

Bingchang Lin[a,b,1], Tong Yun[a,c], Guoming Zhong[a,b], Georges Guiochon[a,b,*]

[a] *Division of Chemical and Analytical Sciences, Oak Ridge National Laboratory, Oak Ridge, TN 37831-6120, USA*

[b] *Department of Chemistry, University of Tennessee, Knoxville, TN 37996-1600, USA*

[c] *Department of Chemical Engineering, University of Tennessee, Knoxville, TN 37996-1600, USA*

First received 30 September 1994; revised manuscript received 13 February 1995; accepted 20 March 1995

Abstract

The onset of the nonlinear behavior of band profiles in elution chromatography is investigated by studying the profile of the shock layer caused by a finite mass transfer resistance in the absence of axial dispersion for a single component. A closed-form analytical expression of the shock layer is obtained for a parabolic isotherm. This solution depends on a dimensionless number which may be used to characterize the degree of nonlinear behavior of the band profiles and to select the model most appropriate for their accurate description. The profiles resulting from this solution are compared with those obtained by numerical calculations under different conditions to assess the influence of the assumptions made. The differences observed illustrate the sensitivity of the elution profiles to small changes in the equilibrium isotherm.

1. Introduction

The single-component elution problem in nonlinear elution chromatography has been abundantly studied [1]. The ideal model predicts the band profile for any isotherm by supplying the equations for the diffuse boundary [1–3], the position of the concentration discontinuity [1,4], and when the isotherm has an inflection point, the various features of the more complex profile [5,6]. This model, however, assumes the column efficiency to be infinite. In practice, this is not so. It has been shown that, provided the column efficiency exceeds a few thousands plates, the profile of the diffuse boundary does not differ significantly from the profile derived from the ideal model [1,7–9], except near the two ends of this profile. This result validates the classical ECP (elution by characteristic points) method of isotherm determinations [10,11], with proper qualifications [1,7–9]. Nevertheless, a vexing problem remains for the theoreticians. In the general elution case, the shock layer which replaces the discontinuity of the ideal model cannot be properly accounted for by an analytical, closed-form equation.

This shock layer arises from the smoothing effects due to axial dispersion and to the resistance to mass transfer across the column. These phenomena prevent the formation of a concentration discontinuity or shock, which in their absence would result from a nonlinear isotherm.

* Corresponding author.

[1] Present address: Iron and Steel Institute, Anshan, Liaoning, China.

0021-9673/95/$09.50
SSDI 0021-9673(95)00380-0

Instead, the dynamic competition between these dispersive phenomena and the self-sharpening influence of a nonlinear isotherm causes the formation of a shock layer with a finite thickness. The resulting band profile can be accounted for properly by using either the equilibrium-dispersive model or a kinetic model [1]. The former model lumps the effect of axial dispersion and mass transfer kinetics into a single apparent axial dispersion term. The latter offers the possibility to handle separately axial dispersion and mass transfer kinetics. The breakthrough profiles in frontal chromatography and the profiles of the band boundaries in the isotachic train of displacement chromatography have been calculated using these models [1,12–17], in the displacement case only for a Langmuir isotherm. Thus, the influence of axial dispersion and the mass transfer resistance can be studied directly, experimental results can be compared in detail to the results of computer calculations, and optimum conditions may be predicted accurately [12–17].

This success is possible, however, because in these two cases, breakthrough curves and profiles of zones of the isotachic train, constant states arise both before and after the profile. A constant pattern takes place between these constant states and the concentration signal tends rapidly towards a steady-state profile which propagates unchanged [1,12–14]. In elution chromatography, by contrast, there is no such constant pattern. The height of the elution band decreases constantly during its migration. Accordingly, the shock propagation velocity changes. It decreases continuously in the case of a convex-upward isotherm. For this reason, it is not possible to derive an analytical solution of the problem in the general case. However, an exact solution of the elution band profile has been derived by Thomas [18] in the case of a Langmuir isotherm, Langmuir kinetics of adsorption/desorption, and no axial dispersion. The solution has been reduced to an analytical equation by Goldstein [19] in the case of a rectangular injection and simplified by Wade et al. [20] in the case of a Dirac pulse injection. This would permit the study of the influence of the mass transfer kinetics on the shock layer profile and on its thickness if the solutions, which include first-order modified Bessel functions of the first kind, were not so complicated and difficult to use. An investigation of the possible use of this solution to derive an analytical expression for the thickness of the shock layer is in progress [21].

It has been long known that an approximate analytical solution of the equilibrium-dispersive model can be derived for weakly nonlinear systems, using a simplified Langmuir isotherm (parabolic isotherm) [22–25]. As the equation obtained is the approximate solution [1,26] of a simplified model, it cannot be used to study the shock layer thickness. However, we have found that, using a variant of these old, conventional models, it is easy to derive a simple equation for the shock layer profile and its thickness without introducing any mathematical approximations. The model itself includes two restrictive, physical conditions, a parabolic isotherm and a minimum column efficiency. This solution permits the study of the influence of the mass transfer kinetics on the formation, profile, and thickness of the shock layer during the onset of column overloading. The results illustrate the passage from linear to nonlinear behavior.

2. Theoretical

Assuming a parabolic isotherm, which is valid in the low concentration range, Houghton [22] and Haarhoff and van der Linde [23] have derived solutions of the equilibrium-dispersive model, in which constant equilibrium between the two phases of the system is postulated, and the band broadening effect of a finite mass transfer kinetics is accounted for by lumping it into an apparent dispersion coefficient which replaces axial dispersion [1]. The derivation of the concentration profile from the system of equations of the model cannot be done without introducing a simplifying assumption [1,22,23]. In the Houghton solution [22], this assumption modifies the mass balance equation in such a way that the mass conservation is destroyed and the

area of the resulting profile depends on the sample size. Other assumptions do not have this inconvenience [23,26].

We show that a rigorous solution can be obtained simply for a model using the parabolic isotherm, neglecting axial dispersion and assuming a finite rate of mass transfer. This kinetic model uses the solid-film linear driving force model. Thus, it is different from the Thomas model [18] which uses the Langmuir kinetics.

2.1. System of equations

Since we neglect axial dispersion due to molecular diffusion and eddy diffusion, the mass balance equation is the same as in the ideal model [1]

$$\frac{\partial C}{\partial t} + F\frac{\partial q}{\partial t} + u\frac{\partial C}{\partial z} = 0 \tag{1}$$

where C and q are the liquid and solid phase concentrations of the component, respectively, t and z are the time and the position in the column, respectively, F is the phase ratio [$F = (1-\varepsilon)/\varepsilon$, where ε is total column porosity], and u is the mobile phase flow velocity.

The mass transfer between the liquid phase and the solid phase is characterized by a simple lumped kinetic equation. We use here the solid-film linear driving force model, written as follows [1],

$$\frac{\partial q}{\partial t} = k(q^* - q) \tag{2}$$

where k is the mass transfer coefficient and q^* is the equilibrium concentration given by the isotherm equation. Most theoretical studies done in chromatography assume a Langmuir isotherm model

$$q^* = \frac{aC}{1+bC} \tag{3a}$$

where a and b are numerical parameters. When bC is negligible, this model reduces to a linear isotherm. When bC is small but no longer negligible, the model can be approximated by a parabolic or second-order Taylor expansion

$$q^* = aC(1-bC) \tag{3b}$$

This situation corresponds to the onset of column overloading, when the effect of a nonlinear isotherm begins to influence the band profile. The similarities and differences between the three isotherms, $q^* = aC$ and Eqs. 3a and 3b, are illustrated in Fig. 1 showing plots of q^* versus bC. The difference between the Langmuir and the linear isotherms is 1% for $bC = 0.01$. The difference between the Langmuir and the parabolic isotherm is 1% for $bC = 0.10$. The parabolic isotherm is meaningless for $bC > 0.5$ because then q^* decreases with increasing C.

The initial and boundary conditions of the problem corresponding to an empty column and to the injection of a very narrow rectangular pulse of feed (Dirac pulse), respectively. These conditions are

$$C(x,0) = 0 \quad 0 < z \tag{4a}$$

$$C(0,t) = C_0 \quad 0 < t \leq t_p \tag{4b}$$

$$C(0,t) = 0 \quad t_p < t \tag{4c}$$

where C_0 is the component concentration in the injected sample and t_p is the injection duration assumed to be very short.

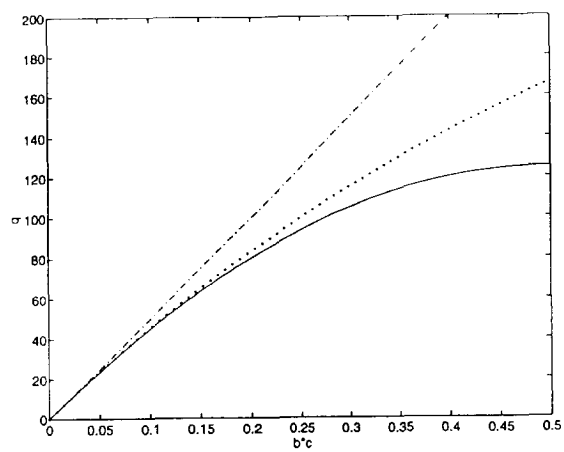

Fig. 1. Comparison of the three equilibrium isotherms: (– · – · –) linear isotherm, $q^* = aC$; (——) parabolic isotherm, $q^* = aC(1-bC)$; (· · · · ·) Langmuir isotherm, $q^* = aC/(1+bC)$. Plot of q^* versus bC. $a = 12$, $b = 0.024$ ml/mg.

2.2. Derivation of the analytical solution of the model

In most practical cases, the column efficiency achieved in preparative chromatography is large, i.e., it largely exceeds a hundred theoretical plates. In such cases, the mass transfer coefficient, k, is relatively large and the deviation of the stationary phase concentration from the equilibrium concentration remains small. Making this assumption, we can rearrange Eq. 2 as follows

$$q = q^* - \frac{1}{k}\frac{\partial q}{\partial t} \approx q^* - \frac{1}{k}\frac{\partial q^*}{\partial t} \tag{5a}$$

For moderate concentrations (i.e., when bC is small), and assuming the isotherm in Eq. 3b, we have

$$q \approx q^* - \frac{a}{k}\frac{\partial C}{\partial t} \tag{5b}$$

Combination of Eqs. 1 and 5b gives

$$\frac{\partial C}{\partial z} + \frac{1 + Fa(1-2bC)}{u}\frac{\partial C}{\partial t} = \frac{Fa}{uk}\frac{\partial^2 C}{\partial t^2} \tag{6}$$

Using the coordinate transform

$$\tau = \frac{1+Fa}{2Fab}\left(z - \frac{u}{1+Fa}t\right) \tag{7}$$

Eq. 6 can be rewritten as

$$\frac{\partial C}{\partial z} - C\frac{\partial C}{\partial \tau} = D_k\frac{\partial^2 C}{\partial \tau^2} \tag{8}$$

with $D_k = u/(4Fab^2k)$. Eq. 8 is Burger's equation. Comparing it to the similar equation derived by Houghton [22] shows that D_k is a diffusion coefficient in the τ domain.

After the coordinate transform (Eq. 7), the initial and boundary conditions become

$$C(z,0) = 0 \quad 0 < z \tag{9a}$$

$$C(0,\tau) = C_0 \quad -\frac{u}{2\,Fab}t_p < \tau < 0 \tag{9b}$$

$$C(0,\tau) = 0 \quad \tau \leqslant -\frac{u}{2\,Fab}t_p \tag{9c}$$

The solution of the classical Burger's equation for the classical Dirac boundary condition is

$$C(z,\tau) = \sqrt{\frac{2S}{\pi R_k z}}\frac{\exp(-w^2)}{\coth(R_k/2) + \mathrm{erf}(w)} \tag{10}$$

with

$$w = \frac{\tau}{\sqrt{2Sz/R_k}} = \frac{\tau}{2\sqrt{D_k z}} \tag{10b}$$

$$S = \frac{uC_0t_p}{2\,Fab} \tag{10c}$$

$$R_k = \frac{S}{2D_k} = C_0t_pbk \tag{10d}$$

A solution for the boundary conditions of a wide injection (Eqs. 9b and 9c) could be easily derived following the same procedure as described by Haarhoff and van der Linde [23]. The following discussion is thus limited to Eq. 10.

No mathematical simplifications have been made to derive a solution of Eq. 8 so Eq. 10 is an exact solution of Eq. 8. It is not an exact solution of the system of equations 1, 2, and 3b, with the initial and boundary conditions in Eqs. 4a–c only because we have assumed that k is large. This restriction does not affect the mass conservation properties of Eq. 1, however, and the profile given in Eq. 10 does conserve the mass. Its area is proportional to the sample size.

The solution obtained is very similar to the profile derived by Haarhoof and van der Linde [23]. The equations giving the band profiles as supplied by the two models can be identified simply, providing a relationship of equivalence between the apparent dispersion coefficient of an equilibrium-dispersive model and the rate coefficient of an equilibrium-transport model giving the same band profile. This relationship is equivalent to the classical expression of the contribution of the finite rate of mass transfer to the column plate height derived by Van Deemter [27]:

$$k = \frac{k_0'}{(1+k_0')^2}\frac{u^2}{D_a} \tag{11}$$

Thus, while the influence on the band profile of the mass transfer resistance can be accounted for correctly by a contribution to the apparent dispersion coefficient of an equilibrium-disper-

sive model, the axial dispersion can be accounted for by a suitable contribution to the rate coefficient of an equilibrium-transport model. This result is another illustration of the equivalence of these models at moderate or high column efficiency [1,26].

2.3. Derivation of the shock layer thickness

Obviously, when k becomes infinite, there is instantaneous equilibrium between the two phases and the model becomes identical to the ideal model. When $R_k \rightarrow \infty$, Eq. 10 can be rewritten as follows

$$C(z,\tau) = \frac{\tau}{z} \quad 0 < t_s < 1 \tag{12a}$$

$$C(z,\tau) = 0 \quad t_s < 0, \quad \text{or} \quad t_s > 1 \tag{12b}$$

where $t_s = \tau/\sqrt{2Sz} = w\sqrt{R_k}$ (Eq. 10b).

This solution is equivalent to the solution of the ideal model, when the concentration is small and the second order terms are neglected. Eq. 12 shows that for any fixed z (e.g. at the column outlet where $z = L$), the concentration jumps from 0 to a maximum concentration given by

$$C_{max} = \frac{\tau}{z}\bigg|_{t_s=1} = \sqrt{\frac{2S}{z}} \tag{13}$$

and which is reached at the time corresponding to $t_s = 1$ or $\tau = \sqrt{2SL}$. Eq. 7 shows that this corresponds to the time

$$t = t_R \equiv \frac{L}{u}\left(1 + Fa - 2\sqrt{\frac{C_0 t_p Fab}{t_0}}\right) \tag{14a}$$

We note that $Fa = k'_0$, the retention factor at infinite dilution, and that the sample size is $n = C_0 t_p F_v = C_0 t_p u S_c$, where F_v is the mobile phase flow-rate and S_c is the cross-sectional area available to the liquid phase. The loading factor of the Langmuir isotherm (Eq. 3a) is $L_f = n/(S_c L F q_s) = (C_0 t_p u)/(L F q_s)$, where q_s is the saturation capacity of the stationary phase, or a/b (Eq. 3a) and S_c is the cross-section area of the column available to the liquid phase. Thus, Eq. 14a is equivalent to

$$t_R = t_0 + k'_0 t_0(1 - 2\sqrt{L_f}) \tag{14b}$$

which is equivalent to the equation giving the retention time of the concentration discontinuity in the case of the ideal model for a Langmuir isotherm $[t_R = t_0 + (t_{R,0} - t_0)(1 - \sqrt{L_f})^2$, [1,4]], where $(1 - \sqrt{L_f})^2$ has been replaced by $(1 - 2\sqrt{L_f})$, a simplification which is valid when L_f is small. Similarly, the concentration becomes 0 again when $\tau = 0$, which corresponds (Eq. 7) to $t = (1 + Fa)L/u = t_0(1 + k'_0) = t_{R,0}$, where $t_{R,0}$ is the retention time at infinite dilution. In the interval between t_R and $t_{R,0}$, the concentration decreases linearly with increasing time, from C_{max} (Eq. 13) to 0. The equation can be rewritten by solving Eq. 7 for t

$$t = t_0(1 + k'_0(1 - 2bC)) \tag{15a}$$

This is the classical simplification of the equation of the ideal model

$$t = t_0\left(1 + \frac{k'_0}{(1 + bC)^2}\right) \tag{15b}$$

for C small. This ideal profile is represented in Fig. 2 for large value of k.

In practice, the mass transfer kinetics is not infinitely fast but k is finite and the mass transfer resistance makes the whole band profile more

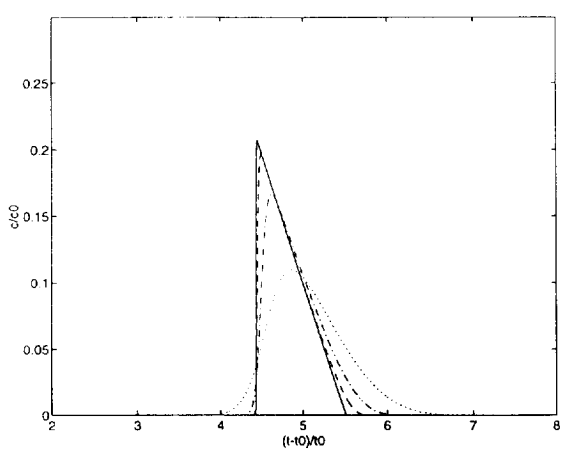

Fig. 2. Comparison of the band profiles obtained with the ideal model and with the equilibrium-transport model discussed here. Parabolic isotherm, parameters as in text and in Figs. 1 and 3. $C_0 = 10$ mg/ml, $t_p = 10$ s. Solid line: ideal model profile, $k = \infty$. Dashed line, $k = 10.0\,s^{-1}$. Chain-dotted line, $k = 2.0\,s^{-1}$. Dotted line, $k = 0.2\,s^{-1}$.

diffuse. The front shock at $t_s = 1$ is replaced by a shock layer, the maximum concentration of the band is less than the ideal value $C_{max} = \sqrt{2S/L}$, and the rear diffuse boundary of the band is no longer a straight line but a curved line which tends toward a Gaussian curve for small values of k. This effect is illustrated in Fig. 2.

When k, hence R_k, is finite, the shock layer can be studied using Eq. 10. When t_s is close to unity, C may be approximated by

$$C(z,\tau) \approx \frac{\tau}{z} \frac{1}{1 + 2\sqrt{\pi R_k} \exp[2R_k(t_s - 1)]} \quad (16)$$

Eq. 16 gives the profile of the band between its beginning ($C = 0$ at $t_s \gg 1$ or $\tau \gg \sqrt{2Sz}$) and its maximum (reached at $t_s = 1$, Eq. 13), i.e., the profile of the shock layer. As C must remain finite, $|2R_k(t_s - 1)|$ also must be finite. Thus, $|t_s - 1|$ is of the same order of magnitude as R_k^{-1} and the order of magnitude of the shock layer thickness is $O(R_k^{-1})$.

The thickness of the shock layer can be derived as the distance between the time of the band beginning ($t_s > 1$) and the time of the band maximum $t_s = 1$. The elution band profile does not begin at any given time, however. Since we are interested in the part of the profile where the concentration is significantly different from 0, we consider the shock layer as the part of the profile front extending between the concentrations C and C_s, with $\theta = C/C_{max}$; θ is chosen arbitrarily, as most convenient for the problem studied (e.g., $\theta = 0.05$ [12,13]). Solving Eq. 16 gives

$$|\Delta t_s| \equiv |t_s - 1| = \frac{1}{2R_k} \log\left(\frac{1}{2\sqrt{\pi}\, R_k} \frac{1-\theta}{\theta}\right) \quad (17a)$$

Replacing t_s by its definition as a function of time gives finally

$$|\Delta t| = \frac{1}{k\sqrt{L_f}} \log\left[\frac{1}{2\sqrt{\pi} L_f S t k_0'} \frac{1-\theta}{\theta}\right] \quad (17b)$$

where $R_k = L_f\, St\, k_0'$ (see Eq. 10d and the definition of the loading factor L_f corresponding to the Langmuir isotherm associated with Eq. 3) and $St = kL/u$ is the Stanton number.

Eq. 17 shows that the thickness of the shock layer is inversely proportional to the kinetic coefficient, k, and to the square root of the loading factor, if we neglect, as a first approximation, the dependence of the logarithmic term on $L_f St$. In frontal analysis and in the isotachic train of displacement chromatography, the shock layer is also proportional to the column HETP [12–17].

2.4. Numerical calculations

Numerical calculations were performed when needed using a classical finite difference method for the integration of the system of equation of the kinetic model, the Godunov or Forward–Backward scheme (Ref. [1], Ch. X). This choice is justified by the fact that Eq. 1 is an Euler equation, including convection but no dispersion. Then, the numerical method gives a stable solution. Its accuracy is only of the first order but this inconvenience is compensated by the rapidity of the calculations. In order to eliminate the band broadening and smoothing effects of numerical dispersion the latter is cancelled by choosing a value of 1.000 001 for the Courant number of the problem [1].

3. Comparison and discussion

In order to illustrate the theoretical results obtained and to study the range of validity of the results derived from the analytical solution of the model (Eqs. 10, 16, and 17), numerical calculations have been performed with a program implementing the solution of the system of Eqs. 1 to 4. Numerical calculations have also been done for a similar model including a dispersive term in Eq. 1. A comparison between the analytical solution of the model and the numerical solutions obtained with either the parabolic or the Langmuir isotherms is discussed later in this section.

The values of the parameters used for the numerical solutions discussed in these comparisons and shown in the figures are: phase ratio, $F = 0.45$; flow velocity, $u = 0.19$ cm/s; column length, $L = 25$ cm; Langmuir isotherm parame-

ters, $a = 12$ and $b = 0.024$ ml/mg, hence $k'_0 = 5.4$ and $q_s = a/b = 500$ mg/ml.

3.1. Effects of the injection concentration

Fig. 3 compares the analytical solution of the simple, nondispersive model derived in the theoretical section with the numerical solution of the same model, using either a parabolic isotherm (Fig. 3a) or a Langmuir isotherm (Fig. 3b), and no axial dispersion term in either cases. This comparison is illustrated for different injection concentrations, C_0, 0.5, 2.0, 10.0, and 20.0 mg/ml. With $t_p = 10$ s, this corresponds to values of the loading factor, L_f, equal to 0.0169%, 0.068%, 0.34%, and 0.68%, respectively, and values of the parameter R_k equal to 0.58, 2.31, 11.6, and 23.1, respectively. The value chosen for the mass transfer kinetics coefficient is $k = 5.0\ s^{-1}$ in all cases, hence a Stanton number, $St = Lk/u$, equal to 657.

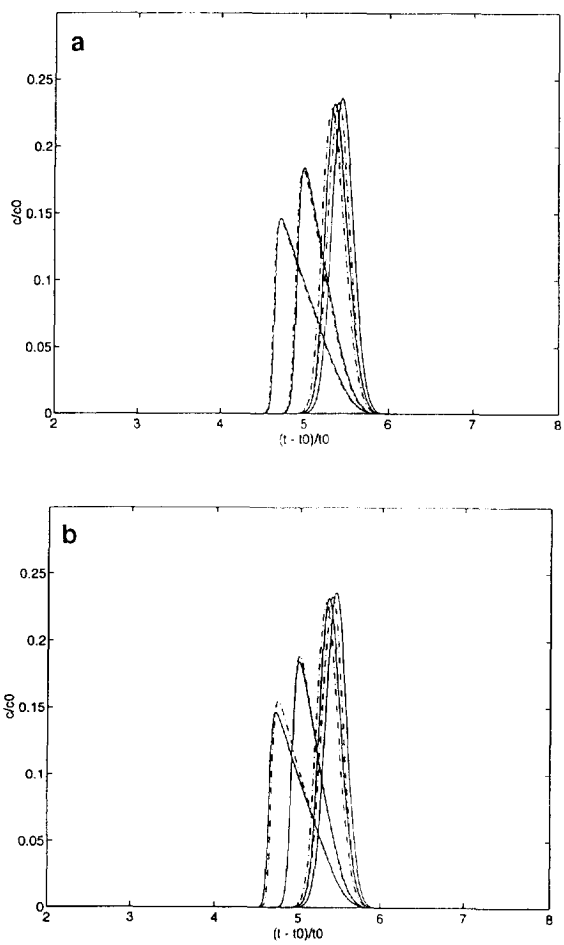

Fig. 3. Comparison between the analytical (solid line) and numerical (chain-dotted line) solutions of the model obtained for different injection concentrations. Feed concentration, $C_0 = 1$, 0.5; 2, 2.0; 3, 10.0; 4, 20.0 mg/ml. In all cases, $t_p = 10$ s; mass transfer coefficient, $k = 5.0\ s^{-1}$; phase ratio, $F = 0.45$; flow velocity, $u = 0.19$ cm/s; column length, $L = 25$ cm; Langmuir isotherm parameters, $a = 12$ and $b = 0.024$ ml/mg. The analytical solution is always obtained for the parabolic isotherm $q = aC(1 - bC)$. (a) The numerical solution is obtained with the parabolic isotherm. (b) The numerical solution is obtained with the corresponding Langmuir isotherm.

As expected, the analytical and numerical solutions of the model are almost identical. The slight differences which are observed between the two profiles of each set are due to the small amount of numerical axial dispersion which has to be used in the calculation of the numerical solutions in order to allow for the numerical stability of the algorithm. This difference, hence the inaccuracy of the numerical solution, becomes significant at small injection concentrations. Both the analytical and numerical results show clearly, however, that at low values of the injection concentration, the chromatographic system behaves linearly or nearly so and the band profile is Gaussian. This is the case of the first profile in Fig. 3a for which $bC = 0.012$, $L_f = 0.0169\%$, and $R_k = 0.58$. By contrast, for large values of C_0 as in the cases of the two largest values used for the calculation of the profiles in Fig. 3a, a sharp front or shock layer appears on the front of the band profile. In this case, the influence on the band profile of the nonlinear behavior of the thermodynamics of the phase equilibrium is obviously dominant. These results suggest that when R_k is larger than 2 the column is overloaded and the band profile skewed while when R_k becomes smaller than unity the influence of the curvature of the isotherm becomes rapidly negligible and linear behavior is observed.

A comparison of the profiles in Figs. 3a and 3b shows that the same profiles are obtained with the parabolic and the Langmuir isotherm for the first two profiles ($bC_0 < 0.05$) and that only very

small differences are seen around the band top for the third profile ($bC_0 = 0.24$). In the case of the fourth profile, there is still a great similarity between the two profiles, the Langmuir profile having a slightly longer retention time and a slightly larger height than the parabolic isotherm profile, and having a curved upward diffuse rear boundary while for the parabolic profile this part of the profile is nearly a straight line down to low concentrations where the influence of the mass transfer kinetics becomes again significant. These differences are explained by the larger amount adsorber, q^*, given by the Langmuir isotherm for any solute concentration, as illustrated in Fig. 1.

4.2. Effects of the rate of the mass transfer kinetics

The comparisons of the analytical and numerical solutions in Fig. 3 were done with different values of the loading factor obtained by changing either the injection concentration or the injection time at constant value of the rate constant of mass transfer. The value chosen ($k = 5\ s^{-1}$) corresponds to a contribution of the mass transfer resistance to the column HETP equal to [1] $H = 2k'_0\mu/(k(1 + k'_0)^2) = 0.01$ cm. This gives to the column an efficiency of 2500 theoretical plates, a rather mediocre figure of merit. As shown by Eqs. 10, 16, and 17, the band profile depends also on the mass transfer kinetics. Fig. 4 shows a comparison of the band profiles obtained at constant loading factor ($t_p = 10$ s, $C_0 = 10$ mg/ml, hence, $L_f = 0.33\%$) for different values of the rate coefficient of mass transfer kinetics, k, between 0.5 and 20 s^{-1}. As seen in Fig. 4, there is an excellent agreement between the analytical and numerical solutions for large values of k. For small values, differences arise because the assumption made in writing Eq. 5 (i.e., that k is large enough to permit replacing $\partial q/\partial t$ by $\partial q^*/\partial t$ in Eq. 2) begins to falter. The analytical solution is not valid for small values of k.

For the value of the loading factor selected, $L_f = 0.33\%$, the behavior of the chromatographic system is strongly nonlinear at the largest values of the mass transfer kinetics (k = 10 or 20 s^{-1}). However, there is a considerable erosion of the shock at low values of the rate coefficient and the shock layer becomes quite wide (Fig. 4a). A nearly Gaussian band profile is obtained as in the linear case for $k = 0.5\ s^{-1}$ ($R_k = 1.20$). Note, however, that for the rather low value of $k = 2\ s^{-1}$, corresponding to a column efficiency of 1000 theoretical plates, an obvious self-sharpening effect appears on the front of the band ($R_k = 4.8$). A similar smoothing phenomenon has been reported in the case of the equilibrium-dispersive model, in which case it depends on the

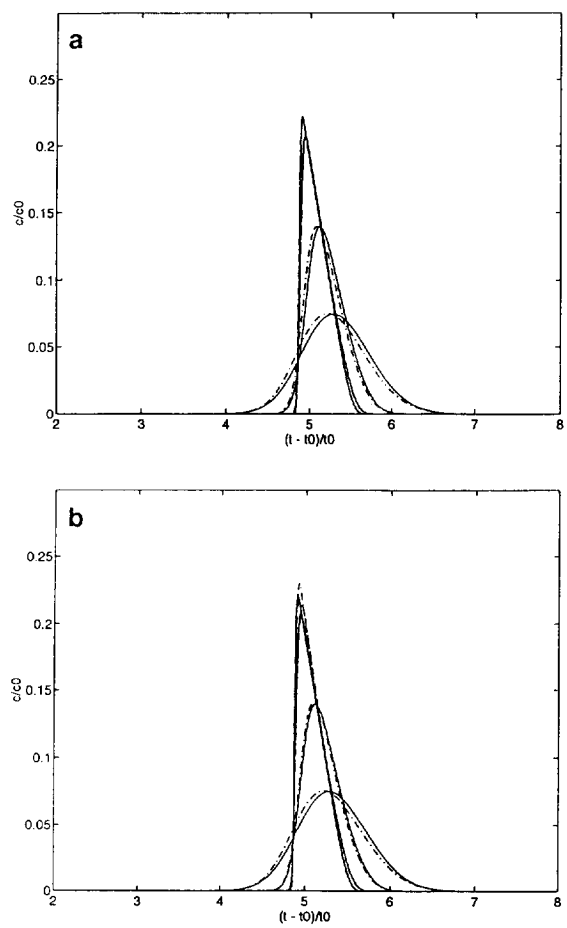

Fig. 4. Comparison between the analytical (solid line) and numerical (chain-dotted line) solutions of the model obtained for different values of the rate coefficient of mass transfer kinetics, k = 1, 0.5; 2, 2.0; 3, 10.0; 4, 20.0 s^{-1}. In all cases, $C_0 = 10$ mg/ml and $t_p = 10$ s. Thus, the loading factor is constant. (a) The numerical solution is obtained with the parabolic isotherm. (b) The numerical solution is obtained with the Langmuir isotherm.

importance of the apparent dispersion coefficient [1]. Fig. 4 shows that the nonlinearity of the chromatographic system is not only controlled by the loading factor, but also by the mass transfer kinetics.

At the end of the Theoretical section, the thickness of the shock layer has been defined and calculated. Applying Eq. 17 to the profiles in Fig. 4a, corresponding to values of k of 0.5, 2, 10, and 20 s^{-1} gives for the shock layer thickness, Δt, 151.2, 49.7, 12.7, and 6.9 s, respectively. The values derived from the numerical solutions are 95.4, 37.4, 9.2, and 5.5 s^{-1}, respectively. As explained above, the difference between the two sets of values observed when the mass transfer kinetics is slow is due to the approximation made in the derivation of Eqs. 5 and 6.

Fig. 4b gives a similar comparison, using the Langmuir isotherm for the calculation of numerical solutions. The results obtained are nearly the same. Except when the mass transfer kinetics is fast, the profiles are quite close. For still lower values of the rate coefficient, the retention time of the band would decrease and the phenomenon of split peaks would eventually appear [1].

4.3. Effects of axial dispersion

The model discussed in the Theoretical section assumes that there is no axial dispersion. In order to estimate the error introduced by neglecting this contribution to band broadening, numerical calculations have been made, using different values of the column Peclet number ($Pe = uL/D_a$, where D_a is axial dispersion coefficient [1]). The numerical solutions calculated with the parabolic and the Langmuir isotherm are shown in Fig. 5a,b, respectively. At large values of Pe, hence high numbers of dispersive stages, the analytical solution gives an excellent approximation of the band profile, for both isotherms.

4.4. Range of validity of the solution

Fig. 6 compares the dependence of the thickness of the shock layer on the rate constant as given by Eq. 16b (solid line) and the value of the shock layer thickness derived from numerical solutions of the kinetic model (symbols). The calculations were performed using a value of the loading factor of 0.7% and a parabolic isotherm, for the sake of consistency. There is an excellent agreement for values of the rate constant between 0.5 and 50 s^{-1}. For low values of the rate constant, the assumption made in the derivation of Eq. 5a is no longer valid. The shock layer predicted by Eq. 16b is too large.

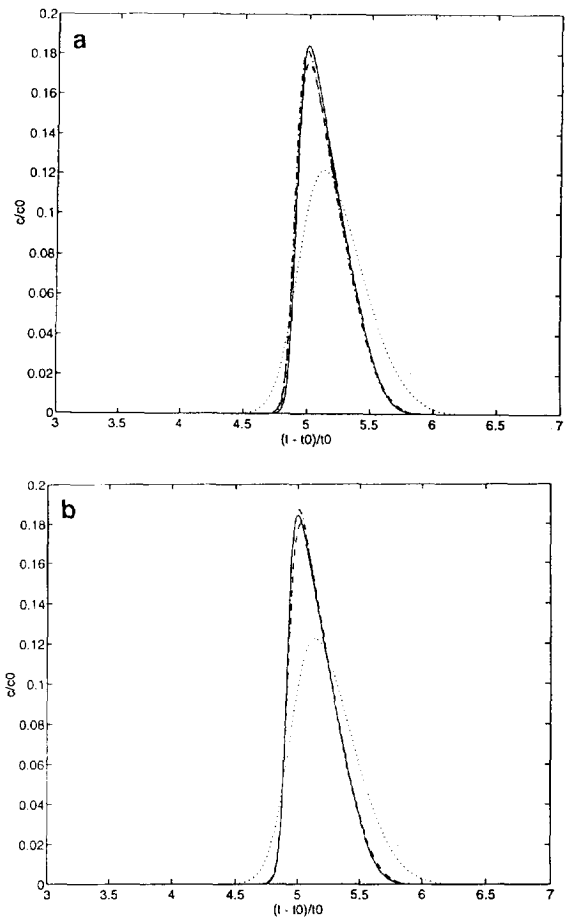

Fig. 5. Comparison between the analytical (solid line) and numerical (chain-dotted line) solutions of the model obtained for different values of axial dispersion, $Pe = 1{,}5000$ (dotted line); 2, 10 000 (dashed line); 3, 30 000 (chain-dotted line). $C_0 = 10$ mg/ml, $t_p = 10$ s and $k = 5.0$ s^{-1}. (a) The numerical solution is obtained with the parabolic isotherm. (b) The numerical solution is obtained with the Langmuir isotherm.

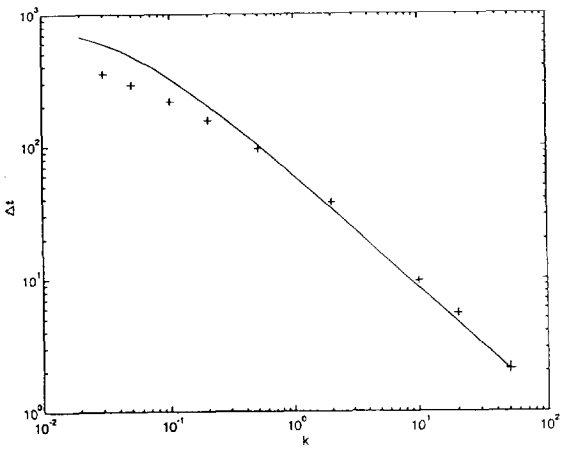

Fig. 6. Comparison between values of the shock layer thickness predicted by Eq. 16b (——) and values derived from a numerical calculation of the band profiles (+).

5. Conclusions

Mass transfer in preparative elution chromatography has been studied. The analytical solution of the band profile, a remained vexing problem, has been given for a parabolic isotherm, also the expression of the shock layer thickness of the band profile due to the mass transfer resistance. The analytical results are compared with numerical simulations using either a parabolic or Langmuir isotherm. The validity of the model is discussed for different value of the parameters.

The value of the dimensionless parameter R_k determines the degree of overloading of the column. If R_k is well below 1, the column is operated under linear conditions. If R_k is larger than unity, the column is overloaded and the band profiles are given by the equations of nonlinear chromatography. From the results displayed in the figures of the present paper, it is clear that the shift takes place in a surprisingly narrow range of values of R_k. The exact nature of this parameter and its fundamental basis require further investigations. It is interesting to note, however, that it is equal to the effective loading factor [1,26,28], m given by

$$m = N\left(\frac{k'_0}{1+k'_0}\right)^2 L_f \tag{18a}$$

Under linear conditions, the contribution of mass transfer resistance to the height equivalent to a theoretical plate, the only contribution in our model, is given by the van Deemter equation [27]

$$H = \frac{2k'_0 u}{k(1+k'_0)^2} \tag{18b}$$

Replacing N in Eq. 18a by L/H, with H as in Eq. 18b gives

$$m = \frac{Lk}{2u} k'_0 L_f = \frac{R_k}{2} \tag{18c}$$

The apparent loading factor has already been used in empirical studies of column overloading. It was implicit in the work of Haarhoff and van der Linde [23] but was used first by De Jong et al. [29] and by Knox and Pyper [30] to characterize the degree of column overloading and compare the behavior of columns with different characteristics. Later Eble et al. [31] showed that there is a universal correlation between the value of m and the ratio N/N_0 of the column efficiencies with the finite sample size, m, and with an infinitely small sample size, at least provided that the equilibrium isotherm is close to a Langmuir isotherm.

As shown by Golshan-Shirazi and Guiochon [1,26,28], the band profile of an actual column, with a finite efficiency (due a finite value of the apparent dispersion coefficient) becomes very close to the profile predicted by the ideal model (column efficiency infinite) if m is larger than 35. We have shown here that the band profile becomes very close to the profile predicted by the linear model if $R_k = 2m$ is lower than 1.

Thus, it seems that we have found a universal parameter which permits a rapid decision regarding the choice of the best model needed to represent or calculate the chromatograms obtained under any set of experimental conditions:
- If $m < 0.5$, the linear model;
- If $0.5 < m < 35$, the equilibrium-dispersive model or a lumped kinetic model, depending on

the column efficiency (if $N > 2000$ the equilibrium-dispersive model should be preferred) and on the relative values of Pe and St. If Pe is large and both N and St small, a lumped kinetic model is needed.
– If $m > 35$, the ideal model.

Acknowledgements

This work has been supported in part by Grant CHE-9201663 of the National Science Foundation and by the cooperative agreement between the University of Tennessee and the Oak Ridge National Laboratory. We acknowledge support of our computational effort by the University of Tennessee Computing Center. We thank the Chinese National Science Foundation (Beijing, PRC) for the Travel Award received by BL.

List of symbols

a first numerical parameter of the isotherm
b second numerical parameter of the isotherm
C liquid phase concentration of the component
C_{max} maximum band concentration
C_0 component concentration in the injected sample
F phase ratio $[F = (1 - \varepsilon)/\varepsilon]$
F_v mobile phase flow-rate
k mass transfer coefficient
L column length
L_f loading factor $[n/(S_c F q_s) = (C_0 t_p u)/(LFq_s)]$
n sample size $(n = C_0 t_p F_v)$
Pe Peclet number $(Pe = uL/D_m)$
q solid phase concentration of the component
q^* equilibrium concentration given by the isotherm equation
q_s saturation capacity of the stationary phase $(q_s = a/b)$
R_k parameter characterizing the sample size $(R_k = \frac{s}{2D_k} = C_0 t_p bk = L_f Stk'_0)$
S_c cross-section area of the column available to the liquid phase
St Stanton number $(St = kL/u)$
t time
t_p injection duration
t_s dimensionless time for the elution profile $(t_s = \tau/\sqrt{2Sz})$
u mobile phase flow velocity
z position in the column

Greek symbols

Δt shock layer thickness for θ
ε total column porosity
θ defines the fractions of the maximum concentration of the band used to measure the shock layer thickness
τ new coordinate $(\tau = \frac{1+Fa}{2Fab}\ (z - \frac{u}{1+Fa}\ t)$

References

[1] G. Guiochon, S. Golshan-Shirazi and A.M. Katti, Fundamentals of Preparative and Nonlinear Chromatography, Academic Press, Boston, MA, 1994, Chapters VII, X, and XIV.
[2] D. DeVault, J. Am. Chem. Soc., 65 (1943) 532.
[3] E. Glueckauf, Proc. Roy. Soc. (London), A186 (1946) 35.
[4] S. Golshan-Shirazi and G. Guiochon, J. Phys. Chem., 94 (1990) 495.
[5] E. Glueckauf, Disc. Faraday Soc., 7 (1949) 12.
[6] J. Hong, Bioprocess Technol., 9 (1990) 495.
[7] R.G. Gerritse and J.F.K. Huber, J. Chromatogr., 71 (1972) 173.
[8] J.F.K. Huber and R.G. Gerritse, J. Chromatogr., 58 (1971) 137.
[9] H. Guan, B.J. Stanley and G. Guichon, J. Chromatogr. A, 659 (1994) 27.
[10] E. Glueckauf, Trans. Faraday Soc., 51 (1955) 1540.
[11] E. Cremer and G.H. Huber, Angew. Chem., 73 (1961) 461.
[12] H.-K. Rhee, B.F. Bodin and N.R. Amundson, Chem. Eng. Sci., 26 (1971) 1571.
[13] H.-K. Rhee and N.R. Amundson, Chem. Eng. Sci., 27 (1972) 199.
[14] T. Vermeulen, M.D. LeVan, N.K. Hiester and G. Klein, in Handbook of Chemical Engineering, Perry Ed., 6th ed., 1984, Ch. 16.
[15] J. Zhu and G. Guiochon, J. Chromatogr., 636 (1993) 189.
[16] J. Zhu, Z. Ma and G. Guiochon, Biotechnol. Progr., 9 (1993) 421.

[17] J. Zhu and G. Guiochon, A.I.Ch.E. J., 41 (1995) 45.
[18] H.C. Thomas, J. Am. Chem. Soc., 66 (1944) 1664.
[19] S. Goldstein, Proc. Roy. Soc. (London), A219 (1953) 151.
[20] J.L. Wade, A.F. Bergold and P.W. Carr, Anal. Chem., 59 (1987) 1286.
[21] G. Zhong and G. Guiochon, in preparation.
[22] G.J. Houghton, J. Phys. Chem., 67 (1963) 84.
[23] P.C. Haarhoff and H.J. Van der Linde, Anal. Chem., 38 (1966) 573.
[24] A. Jaulmes, C. Vidal-Madjar, A. Ladurelli and G. Guiochon, J. Phys. Chem., 88 (1984) 5379.
[25] A. Jaulmes, C. Vidal-Madjar, H. Colin and G. Guiochon, J. Phys. Chem., 90 (1986) 207.
[26] S. Golshan-Shirazi and G. Guiochonu, J. Chromatogr., 506 (1990) 495.
[27] J.J. van Deemter, F.J. Zuiderweg and A. Klinkenberg, Chem. Eng. Sci., 5 (1956) 271.
[28] S. Golshan-Shirazi and G. Guiochon, Anal. Chem., 61 (1989) 462.
[29] A.W.J. De Jong, H. Poppe and J.C. Kraak, J. Chromatogr., 148 (1978) 127.
[30] J.H. Knox and H.M. Pyper, J. Chromatogr., 363 (1986) 1.
[31] J.E. Eble, R.L. Grob, P.E. Antle and L.R. Snyder, J. Chromatogr., 384 (1987) 45.